Information Sciences 569 (2021) 669–686

Contents lists available at ScienceDirect

Information Sciences

journal homepage: www.elsevier.com/locate/ins

Adapting H-infinity controller for the desired reference tracking of the sphere position in the maglev process

José de Jesús Rubio [a,*], Edwin Lughofer [b], Jeff Pieper [c], Panuncio Cruz [a], Dany Ivan Martinez [a], Genaro Ochoa [a], Marco Antonio Islas [a], Enrique Garcia [a]

[a] Sección de Estudios de Posgrado e Investigación, Esime Azcapotzalco, Instituto Politécnico Nacional Av, de las Granjas no. 682, Col. Santa Catarina, México City 02250, Mexico
[b] Department of Knowledge-Based Mathematical Systems, Johannes Kepler University Linz, Linz, Austria
[c] Department of Mechanical Engineering, University of Calgary, Calgary, Canada

ARTICLE INFO

Article history:
Received 23 February 2021
Received in revised form 2 April 2021
Accepted 10 May 2021
Available online 18 May 2021

Keywords:
Maglev process
Foucault current
adapting
H-infinity controller
Convergence

ABSTRACT

The Maglev process consists in a magnetic field geerated by the modulation of a coil current which yields the sphere levitation. Foucault current is the current transmitted from the coil to a sphere in the Maglev process which yields the undesired sphere vibrations. In this study, an adapting H-infinity controller is introduced as the combination of the adapting and H-infinity strategies for the desired reference tracking of the sphere position in the Maglev process. The adapting strategy is used for the unknown dynamics estimation, and the H-infinity strategy is used for the desired reference tracking. The Lyapunov technique is used to satisfy the error convergence and the H-infinity criterion. Two simulations show the effectiveness of the considered method for the desired reference tracking of the sphere position in the Maglev process.

1. Introduction

The Maglev process consists in a magnetic field generated by the modulation of a coil current which yields the sphere levitation. It is explained by two steps: 1) a voltage is induced in the coil to generate a varying magnetic flux, 2) the induced voltage yields a current from the coil to the sphere known as the Foucault current. The Foucault current yields undesired sphere vibrations which can prevent the Maglev process from reaching near a steady state final value; consequently, a controller must be required to reach the error convergence in the desired reference tracking of the sphere.

There are some controllers applied to Maglev processes. In [1–4] fuzzy controllers, in [5–8] H-infinity controllers, in [9–12] nonlinear controllers, and in [13–18] sliding mode controllers are focused on the Maglev process. The above mentioned results show that the Maglev process is a novel and recent research; consequently, the design of a controller for this process would be of great interest. The Maglev process has three drawbacks: 1) fast movements in the sphere position yield vibrations, i.e., fast movements in the sphere position are not convergent, and 2) an adapting strategy only reaches the estimation of slow dynamics, while the H-infinity technique is primarily aimed at the desired reference tracking of fast dynamics. A proposed solution for all drawbacks in the Maglev process is presented in this research as following: 1) dead-zone adapting laws are introduced in the adapting strategy to estimate unknown dynamics of the sphere position, 2) H-infinity is combined with

* Corresponding author.
E-mail address: rubio.josedejesus@gmail.com (J.J. Rubio).

https://doi.org/10.1016/j.ins.2021.05.018
0020-0255/

the adapting strategy to obtain the desired reference tracking of the sphere position. In this paper, the following two main contributions in a Maglev process are introduced: 1) a model of the Maglev process which considers the Foucault currents is proposed, 2) a convergent adapting H-infinity controller is designed to attenuate the effects of the Foucault currents and to decrease vibrations in the sphere position. The Maglev process has been utilized in induction motors, transport, low friction bearings, energy storage, smelting, high velocity trains, industries, and academics.

The paper is organized as following. In Section 2, the Maglev dynamic model is described. In Section 3, the transformation of the Maglev model is detailed through the utilization of a generalized controller methodology. In Section 4, the adapting H-infinity controller is designed for the desired reference tracking of the sphere position in the Maglev process. In Section 5, the proposed controller is compared with the two stages and robust tracking methods for the desired reference tracking of the sphere position in the Maglev process. Section 6 presents conclusions and forthcoming work.

2. Maglev dynamic model

This section consists in two parts, the Foucault current model, and the Maglev process model.

2.1. Kinematics of the Foucault currents

The goal of this subsection is to show that the power related with the Foucault current will be different from zero; consequently, it will show the existence of the Foucault current in the Maglev process.

The Foucault current is composed of electrons moving in circles due to the movement of a metallic sphere inside of a magnetic field. It is a drawback in the controller of the Maglev processes because the Foucault current creates magnetic fields

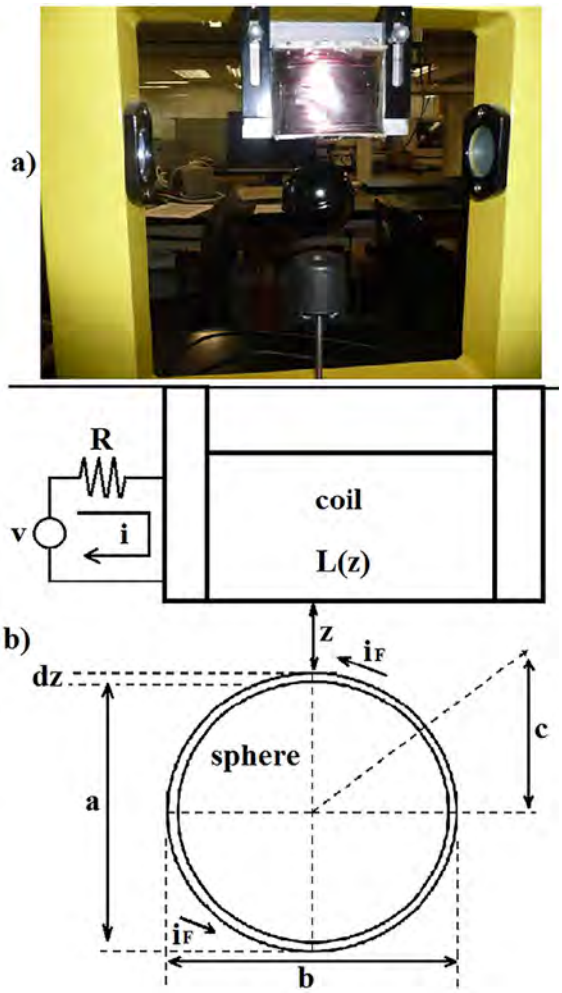

Fig. 1. Foucault current around the sphere in the Maglev process.

which are opposite to the magnetic fields in the coil; consequently, it yields vibrations in the sphere. Some metallic spheres have small holes to attenuate vibrations, but it is difficult to avoid this phenomenon. Fig. 1 shows the flow of the Foucault current around the sphere in the Maglev process which is denoted as i_F.

From Fig. 1, the Foucault current i_F is the electric current moving around the sphere, the sphere has conductivity γ, the magnetic field denoted as B_F yields the Foucault current which is proportional to the velocity of B_F, with $\omega = 2\pi f, z$ is the distance from the coil to the sphere, dz is a variation of z of the vibration due to the Foucault current.

The Foucault current creates magnetic fields in the sphere which obey the Lorenz law. To evaluate this fact, the sphere of Fig. 1 b) is considered with the thickness a, the width b, and the length c, $b > a$. For the desired reference with a distance to the z axis, it is supposed that there is a vibration of width dz and depth c for the transportation of the Foucault current.

Observing the sphere of Fig. 1 b) and assuming negligible extreme effect, the Foucault current i_F is

$$\begin{aligned} i_F &= \tfrac{e_F}{R_F}, \\ R_F &= \tfrac{1}{\gamma}\tfrac{2b}{cdz}, \end{aligned} \tag{1}$$

R_F is the ohmic resistance, e_F is the voltage of the Faraday law as

$$\begin{aligned} e_F &= \tfrac{d\phi_F}{dt} = 2zb\tfrac{dB_F}{dt} = 2zbB_{\max}\omega\cos(\omega t), \\ B_F &= B_{\max}\sin(\omega t), \end{aligned} \tag{2}$$

B_F is the internal magnetic field. Substituting (2) in (1) is

$$i_F = B_{\max}\omega\gamma c(\cos(\omega t))zdz. \tag{3}$$

Power is measured in an entire cycle of the variation of B_F, i.e.; since the period $T = 2\pi\omega$, the power is

$$\begin{aligned} p_i &= \tfrac{1}{T}\int_0^T eid(\omega t) \\ &= 2B_{\max}^2\omega^2\gamma bc(z^2dz)\tfrac{1}{T}\int_0^T \cos^2(\omega t)\dot{d}(\omega t), \\ &\int_0^T \cos^2(\omega t)\dot{d}(\omega t) = \tfrac{T}{2}, \end{aligned} \tag{4}$$

then

$$p_i = B_{\max}^2\omega^2\gamma bcz^2dz. \tag{5}$$

It is the power in the circuit of the thread of width dz, see Fig. 1 b), but to cover the metallic sphere, the power of similar elements have to be added from $z = 0$ to $z = a$, then the total power is

$$\begin{aligned} p_F &= \int_0^a p_i = \int_0^a B_{\max}^2\omega^2\gamma bcz^2dz \\ &= B_{\max}^2\omega^2\gamma bc\tfrac{a^3}{3}. \end{aligned} \tag{6}$$

From (6), the sphere length a has great importance to decrease vibrations due to the Foucault current i_F. If the length of a is smaller, vibrations are smaller, which yields the selection of thin spheres.

2.2. Maglev model

Fig. 1 b) shows that the Maglev process in the coil and sphere. Using Newton's second law, the sphere dynamics of Fig. 1 b) are

$$m\ddot{z} = mg - F_{em}, \tag{7}$$

F_{em} is the electromagnetic force which generates electromagnetic effects, z is the varying distance from the coil to the sphere, $\dot{z}$ is the velocity, and $\ddot{z}$ is the acceleration, m is the mass, and g is the gravity acceleration. The electromagnetic force F_{em} is

$$F_{em} = \frac{L_r}{2a}i^2e^{-\frac{z}{a}}, \tag{8}$$

L_r is the inductance which decreases when the coil is near to the sphere ($z \to 0$) due to the induced Foucault current, i is the coil current. The inductance is a mapping of the coil position z above the sphere, and it decreases with the length a.

Then, substituting the value of the electromagnetic force of (8) into (7) is

$$\ddot{z} = -\frac{L_r}{2am}i^2e^{-\frac{z}{a}} + g. \tag{9}$$

From the coil circuit of Fig. 1 b), the Kirchhoff voltages law is employed to obtain the source voltage υ as

$$\upsilon = Ri + L(z)\frac{di}{dt} + c_i, \tag{10}$$

i is the coil current, υ is the voltage which is a coil source, $L(z)\frac{di}{dt}$ is the coil voltage, Ri is a resistance voltage, R is the coil resistance, c_i is a parameter due to Foucault current i_F, $L(z)$is the coil inductance

$$L(z) = L_0 + L_r e^{-\frac{z}{a}},$$

L_0 is the coil inductance when it is far to the sphere ($z \to \infty$), L_r and a are in (8).

Finally, taking into account the states as $\chi_1 = z, \chi_2 = \dot{z}$, and $\chi_3 = i$, as the position, velocity, and current of the sphere, respectively, and the input $u = \frac{1}{k_i}\upsilon$ of the sphere, considering (9) and (10), yields the dynamic model of the Maglev process as

$$\begin{aligned}
\dot{\chi}_1 &= \chi_2,\\
\dot{\chi}_2 &= -\tfrac{L_r}{2am}\chi_3^2 e^{-\frac{\chi_1}{a}} + g,\\
\dot{\chi}_3 &= \tfrac{k_i u}{L_0 + L_r e^{-\frac{\chi_1}{a}}} - \tfrac{R\chi_3}{L_0 + L_r e^{-\frac{\chi_1}{a}}} + \tfrac{c_i}{L_0 + L_r e^{-\frac{\chi_1}{a}}},\\
y &= \chi_1,
\end{aligned} \tag{11}$$

k_i is a positive constant.

Remark 1. (11) is the main equation to describe the dynamic model of the Maglev process. From (11), the main variables of the Maglev process are the position $\chi_1 = z$, velocity $\chi_2 = \dot{z}$, current $\chi_3 = i$, and input $u = \frac{1}{k_i}\upsilon$ of the sphere, $\chi_1 \in [0, 0.016], \chi_2 \in [-\infty, \infty], \chi_3 \in [0.03884, 2.38]$, $u \in [0, 1]$, $\chi(0)=[\chi_1(0), \chi_2(0), \chi_3(0)]^T$ is the initial condition of $\chi = [\chi_1, \chi_2, \chi_3]^T$ selected by user between the values $\chi_1(0) \in [0, 0.016]$, $\chi_2(0) \in [-500, 500]$, $\chi_3(0) \in [0.03884, 2.38]$.

3. Nonlinear controller design

In this section, a generalized controller methodology is utilized to obtain the transformed Maglev model, which will be required in the subsequent section for controller design.

The nonlinear Maglev process has similar behavior to an approximated linear process in a small range of movement. But the linear controller is damaged very quickly when the nonlinear process falls out of a given range of movement. Consequently, in this section a nonlinear controller is designed by the generalized controller methodology.

Deviation states of the position, velocity, current denoted as $\varsigma\chi_1, \varsigma\chi_2, \varsigma\chi_3$, and the deviation controller denoted as ςu are

$$\begin{aligned}
\varsigma\chi_1 &= \chi_1 - \chi_1^*\\
\varsigma\chi_2 &= \chi_2 - \chi_2^*\\
\varsigma\chi_3 &= \chi_3 - \chi_3^*\\
\varsigma u &= u - u^*
\end{aligned} \tag{12}$$

$\chi_1^*, \chi_2^*, \chi_3^*$ are constant equilibrium points of the position, velocity, current, and u^* is the steady controller.

Taking into account (12), the process of (11) can be written as

$$\begin{aligned}
\varsigma\dot{\chi}_1 &= \varsigma\chi_2 + \chi_2^* = \chi_2,\\
\varsigma\dot{\chi}_2 &= -\tfrac{L_r}{2am}\left(\varsigma\chi_3 + \chi_3^*\right)^2 e^{-\frac{\left(\varsigma\chi_1 + \chi_1^*\right)}{a}} + g,\\
\varsigma\dot{\chi}_3 &= \tfrac{k_i u^*}{L_0 + L_r e^{-\frac{\left(\varsigma\chi_1 + \chi_1^*\right)}{a}}} + \tfrac{c_i}{L_0 + L_r e^{-\frac{\left(\varsigma\chi_1 + \chi_1^*\right)}{a}}}\\
&\quad - \tfrac{R\left(\varsigma\chi_3 + \chi_3^*\right)}{L_0 + L_r e^{-\frac{\left(\varsigma\chi_1 + \chi_1^*\right)}{a}}} + \tfrac{k_i}{L_0 + L_r e^{-\frac{\left(\varsigma\chi_1 + \chi_1^*\right)}{a}}}\varsigma u,\\
\varsigma y &= \varsigma\chi_1 + \chi_1^*.
\end{aligned} \tag{13}$$

The process output is differentiated successively until reaching an equation as a relation of the output and the input. Obtaining the derivatives it is

$$
\begin{aligned}
&\varsigma y = \varsigma\chi_1 + \chi_1^*,\\
&\varsigma\dot{y} = \varsigma\dot{\chi}_1 = \varsigma\chi_2 + \chi_2^*,\\
&\varsigma\ddot{y} = \varsigma\dot{\chi}_2 = -\tfrac{L_r}{2am}\left(\varsigma\chi_3 + \chi_3^*\right)^2 e^{-\frac{\left(\varsigma\chi_1+\chi_1^*\right)}{a}} + g,\\
&\varsigma\cdot\ddot{y} = -\tfrac{L_r}{2am}\left[\left(\varsigma\chi_3 + \chi_3^*\right)^2\left(-\tfrac{1}{a}e^{-\frac{\left(\varsigma\chi_1+\chi_1^*\right)}{a}}\varsigma\dot{\chi}_1\right)\right]\\
&-\tfrac{L_r}{2am}\left[\left(2\left(\varsigma\chi_3 + \chi_3^*\right)\varsigma\dot{\chi}_3 e^{-\frac{\left(\varsigma\chi_1+\chi_1^*\right)}{a}}\right)\right],\\
&= \tfrac{L_r}{2a^2m}\left(\varsigma\chi_2 + \chi_2^*\right)\left(\varsigma\chi_3 + \chi_3^*\right)^2 e^{-\frac{\left(\varsigma\chi_1+\chi_1^*\right)}{a}}\\
&+\frac{L_rR}{am\left(L_0+L_re^{-\frac{\left(\varsigma\chi_1+\chi_1^*\right)}{a}}\right)}\left(\varsigma\chi_3 + \chi_3^*\right)^2 e^{-\frac{\left(\varsigma\chi_1+\chi_1^*\right)}{a}}\\
&-\frac{L_rk_i}{am\left(L_0+L_re^{-\frac{\left(\varsigma\chi_1+\chi_1^*\right)}{a}}\right)}\left(\varsigma\chi_3 + \chi_3^*\right)e^{-\frac{\left(\varsigma\chi_1+\chi_1^*\right)}{a}}u^*\\
&-\frac{L_rk_i}{am\left(L_0+L_re^{-\frac{\left(\varsigma\chi_1+\chi_1^*\right)}{a}}\right)}\left(\varsigma\chi_3 + \chi_3^*\right)e^{-\frac{\left(\varsigma\chi_1+\chi_1^*\right)}{a}}\varsigma u\\
&-\frac{L_rc_i}{am\left(L_0+L_re^{-\frac{\left(\varsigma\chi_1+\chi_1^*\right)}{a}}\right)}\left(\varsigma\chi_3 + \chi_3^*\right)e^{-\frac{\left(\varsigma\chi_1+\chi_1^*\right)}{a}}.
\end{aligned}
\tag{14}
$$

The output is differentiated three times to find the input. This implies that the relative degree of the process is $r = 3$ which is known as a condition required to assure the transformation of inputs-output pairings. Later, the process of Eq. (14) can be rewritten as

$$
\begin{aligned}
&\varsigma y = \varsigma\chi_1 + \chi_1^*,\\
&\varsigma\dot{y} = \varsigma\chi_2 + \chi_2^*,\\
&\varsigma\ddot{y} = -\tfrac{L_r}{2am}\left(\varsigma\chi_3 + \chi_3^*\right)^2 e^{-\frac{\left(\varsigma\chi_1+\chi_1^*\right)}{a}} + g,\\
&\varsigma\cdot\ddot{y} = r(\chi) + s(\chi)\varsigma u + q
\end{aligned}
\tag{15}
$$

with

$$
\begin{aligned}
&r(\chi) = \tfrac{L_r}{2a^2m}\left(\varsigma\chi_2 + \chi_2^*\right)\left(\varsigma\chi_3 + \chi_3^*\right)^2 e^{-\frac{\left(\varsigma\chi_1+\chi_1^*\right)}{a}}\\
&+\frac{L_rR}{am\left(L_0+L_re^{-\frac{\left(\varsigma\chi_1+\chi_1^*\right)}{a}}\right)}\left(\varsigma\chi_3 + \chi_3^*\right)^2 e^{-\frac{\left(\varsigma\chi_1+\chi_1^*\right)}{a}}\\
&-\frac{L_rk_i}{am\left(L_0+L_re^{-\frac{\left(\varsigma\chi_1+\chi_1^*\right)}{a}}\right)}\left(\varsigma\chi_3 + \chi_3^*\right)e^{-\frac{\left(\varsigma\chi_1+\chi_1^*\right)}{a}}u^*,\\
&s(\chi) = -\frac{L_rk_i}{am\left(L_0+L_re^{-\frac{\left(\varsigma\chi_1+\chi_1^*\right)}{a}}\right)}\left(\varsigma\chi_3 + \chi_3^*\right)e^{-\frac{\left(\varsigma\chi_1+\chi_1^*\right)}{a}},\\
&q = -\frac{L_rc_i}{am\left(L_0+L_re^{-\frac{\left(\varsigma\chi_1+\chi_1^*\right)}{a}}\right)}\left(\varsigma\chi_3 + \chi_3^*\right)e^{-\frac{\left(\varsigma\chi_1+\chi_1^*\right)}{a}}.
\end{aligned}
\tag{16}
$$

Remark 2. The objective of this section is to obtain the transformed Maglev process of (15), (16). From (15), (16), the main variables of the transformed Maglev process are ςu and $\varsigma y = \varsigma\chi_1 + \chi_1^*$ are the input and output, χ_1^* is the constant equilibrium point of the position selected by user between the values $\chi_1^* \in [0, 0.016]$, and the steady controller u^* is selected by user between the values $u^* \in [0, 1]$.

4. Adapting H-infinity controller

In this section, an adapting strategy is proposed to estimate the unknown nonlinear mappings and an H-infinity controller is introduced to attenuate the vibrations produced by the Foucault current.

Taking into account the nonlinear process as

$$\varsigma \cdot \ddot{y} = r(\chi) + s(\chi)\varsigma u + q, \tag{17}$$

$r(\chi), s(\chi)$ are unknown nonlinear mappings and q is the vibration parameter due to the Foucault current given in (15), (16). According to the Stone-Weierstrass theorem, the unknown nonlinear mapping q is approximated as

$$q = W^{*}\sigma(\chi) + \xi, \tag{18}$$

W^{*} is an idealized parameter obtained as a result of the training of the adapting strategy. $\sigma(s)$is the nonlinear activation mapping, and ξ describes the unmodelled terms.

The main goal of a controller is that the process output $\varsigma y = \varsigma\chi_1 + \chi_1^{*}$ (15), (16) must reach the bounded desired reference ςy_d, it is known as the desired reference tracking of the sphere position in the Maglev process. Employing the uncertainty δ_c to be defined later, a successful desired reference tracking performance is described by the H-infinity criterion as

$$\lim_{t\to\infty}\frac{1}{t}\int_0^t e_c^T Q_c e_c dt \leqslant \lambda^2 \lim_{t\to\infty}\frac{1}{t}\int_0^t O_\delta^T O_\delta dt, \tag{19}$$

$e_c = \left[\tilde{y}, \dot{\tilde{y}}, \ddot{\tilde{y}}\right]^T$ is the tracking error to be defined later, $O_\delta > 0$ is a positive constant depending of q (17) such as $\delta_c^T\delta_c \leqslant O_\delta^T O_\delta$, O_δ is a positive definite matrix to be defined later, λ is an attenuation parameter which will defined later.

4.1. Desired reference tracking problem

In this section, the controller is augmented with additional variables to compensate some nonlinearities of the Maglev process with the objective to reach the asymptotic error convergence. Consequently, H-infinity and adapting strategies are combined to solve the desired reference tracking problem as in Fig. 2.

For the desired reference tracking of the sphere position in the transformed Maglev process (15), (16), the controller law is proposed as

$$\begin{aligned} u &= u^{*} + \varsigma u, \\ \varsigma u &= \tfrac{1}{\hat{s}(\chi)}\left[-\hat{r}(\chi) + \varsigma\cdot\ddot{y}_d - \zeta^T e_c + u_c\right], \end{aligned} \tag{20}$$

$\chi = \left[\chi_1, \chi_2, \chi_3\right]^T$ are the main variables of the Maglev process (11), $e_c = \left[\tilde{y}, \dot{\tilde{y}}, \ddot{\tilde{y}}\right]^T$ is the tracking error, $\zeta^T = [\zeta_0, \zeta_1, \zeta_2]$ is the proportional gain of the controller such that the polynomial $\cdot\dddot{\tilde{y}} + \zeta_2\ddot{\tilde{y}} + \zeta_1\dot{\tilde{y}} + \zeta_0\tilde{y}$ is Hurwitz, $\tilde{y} = \varsigma y - \varsigma y_d$ is the output tracking error, $\varsigma u = u - u^{*}$ and $\varsigma y = \varsigma\chi_1 + \chi_1^{*}$ are the input and output of the transformed Maglev process (15), (16), u^{*}, χ_1^{*} are selected by user between the values $\chi_1^{*} \in [0, 0.016]$, $u^{*} \in [0, 1]$, ςy_d is the desired reference, $\hat{r}(\chi)$and $\hat{s}(\chi)$are the estimation of unknown

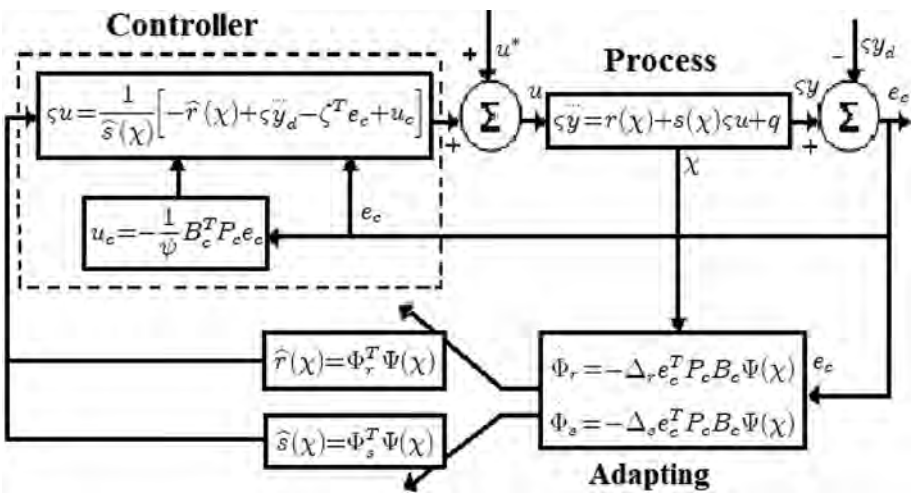

Fig. 2. The adapting H-infinity controller scheme.

nonlinear mappings $r(\chi)$and $s(\chi)$, u_c is the H-infinity controller to be defined later. Defining mappings error as $\tilde{r}(\chi)=\hat{r}(\chi)-r(\chi)$, $\tilde{s}(\chi)=\hat{s}(\chi)-s(\chi)$ and substituting the controller law (20) into the process (17) results in

$$\begin{aligned}
&\varsigma\cdot\ddot{y}=r(\chi)+s(\chi)\varsigma u+q\\
&\varsigma\cdot\ddot{y}=\left(\hat{r}(\chi)-\tilde{r}(\chi)\right)+\left(\hat{s}(\chi)-\tilde{s}(\chi)\right)\varsigma u+q\\
&\varsigma\cdot\ddot{y}=\hat{s}(\chi)\tfrac{1}{\hat{s}(\chi)}\left[-\hat{r}(\chi)+\varsigma\cdot\ddot{y}_d-\zeta^T e_c+u_c\right]\\
&+\hat{r}(\chi)-\tilde{r}(\chi)-\tilde{s}(\chi)\varsigma u+q\\
&\varsigma\cdot\ddot{y}=\varsigma\cdot\ddot{y}_d-\zeta^T e_c+u_c+\delta+q\\
&\Rightarrow\dddot{\tilde{y}}=\varsigma\cdot\ddot{y}-\varsigma\cdot\ddot{y}_d=-\zeta^T e_c+u_c+\delta+q,
\end{aligned}\tag{21}$$

the controller law u_c has the goal to compensate the modelling error δ

$$\delta=-\tilde{r}(\chi)-\tilde{s}(\chi)\varsigma u,\tag{22}$$

The Eq. (21) can be written in states space process as

$$\begin{aligned}
&\dot{e}_c=A_c e_c+B_c u_c+B_c\{\delta+q\},\\
&A_c=\left(A-B_c\zeta^T\right),
\end{aligned}\tag{23}$$

with

$$A=\begin{bmatrix}0&1&0\\0&0&1\\0&0&0\end{bmatrix},B_c=\begin{bmatrix}0\\0\\1\end{bmatrix},\zeta=\begin{bmatrix}\zeta_0\\\zeta_1\\\zeta_2\end{bmatrix},\tag{24}$$

The Eq. (23) describe the desired reference tracking problem. The controller law u_c is the H-infinity controller utilized for the desired reference tracking of the sphere position in the Maglev process as

$$u_c=-\frac{1}{\psi}B_c^T P_c e_c.\tag{25}$$

$B_c=[0,0,1]^T$ is described in (24), ψ is a positive constant selected by user, P_c is a positive definite matrix detailed in the subsequent subsections.

4.2. Estimation of the unknown dynamics in the process

The estimation of the unknown nonlinear mappings $r(\chi)$ and $s(\chi)$ of (17) can be developed with the first order adapting strategy of Fig. 3. The Gaussian mappings can be adapted to the changing behavior of the process as compared to sigmoid mappings for two reasons: 1) the Gaussian mappings have widths and centers while the sigmoid mappings have centers, and 2) the Gaussian mappings can learn positive and negative values, while the sigmoid mappings only can learn positive values.

The estimation of $r(\chi)$ and $s(\chi)$ as the same as [19–24] has the form

$$\begin{aligned}
&\hat{r}(\chi)=\Phi_r^T\Psi(\chi),\\
&\hat{s}(\chi)=\Phi_s^T\Psi(\chi),\\
&\Psi(\chi)=\sum_{l=1}^{n}\mu_{M_l}
\end{aligned}\tag{26}$$

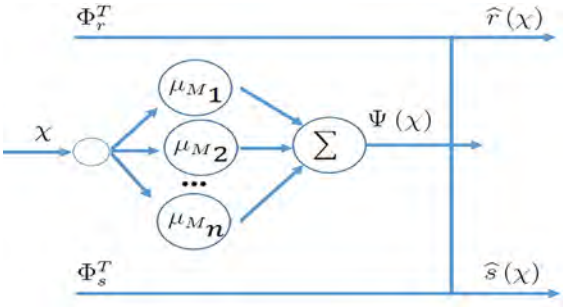

Fig. 3. The adapting compensation.

n is the adapting number, $\Psi(\chi)$ is an adapting mapping, $\mu_{M_l} = e^{-\left(\frac{\chi - c_l}{\sigma_l}\right)^2}$ are Gaussian mappings, c_l are centers, σ_l are widths, $\widehat{r}(\chi), \widehat{s}(\chi)$are outputs of the adapting strategy, $\chi = [\chi_1, \chi_2, \chi_3]^T$. Even $\widehat{r}(\chi)$and $\widehat{s}(\chi)$ have the same structure, they are required because $\widehat{r}(\chi)$ will be used in the numerator and $\widehat{s}(\chi)$will be used in the denominator of a controller law to be defined later. It is assumed that parameters of the adapting strategy denoted as Φ_r and Φ_s are time-varying and bounded by O_{Φ_r} and O_{Φ_s} as

$$\begin{aligned} O_{\Phi_r} &= \{\Phi_r \in \Re : \|\Phi_r\| \leqslant k_{\Phi_r}\}, \\ O_{\Phi_s} &= \{\Phi_s \in \Re : \|\Phi_s\| \leqslant k_{\Phi_s}\}, \end{aligned} \tag{27}$$

k_{Φ_r} and k_{Φ_s} are positive constants. The values of Φ_r and Φ_s yield an optimal estimation

$$\begin{aligned} \Phi_r^* &= \arg \min_{\Phi_r \in O_{\Phi_r}} \left[\sup_{\chi \in U_\chi} |r(\chi) - \widehat{r}(\chi)| \right], \\ \Phi_s^* &= \arg \min_{\Phi_s \in O_{\Phi_s}} \left[\sup_{\chi \in U_\chi} |s(\chi) - \widehat{s}(\chi)| \right]. \end{aligned} \tag{28}$$

Φ_r^* and Φ_s^* are constant parameters of Φ_r and Φ_s to obtain good estimation. The modelling error δ for $r(\chi)$and $s(\chi)$is in (22), and it is discomposed in δ_r and δ_s as

$$\begin{aligned} \delta &= \delta_r + \delta_s, \\ \delta_r &= \tfrac{1}{2}\widetilde{r}(\chi) + \tfrac{1}{2}\widetilde{s}(\chi)\varsigma u, \\ \delta_s &= \tfrac{1}{2}\widetilde{r}(\chi) + \tfrac{1}{2}\widetilde{s}(\chi)\varsigma u. \end{aligned} \tag{29}$$

Finally, the parameters estimation errors $\widetilde{\Phi}_r$ and $\widetilde{\Phi}_s$ are

$$\begin{aligned} \widetilde{\Phi}_r &= \Phi_r - \Phi_r^*, \\ \widetilde{\Phi}_s &= \Phi_s - \Phi_s^*. \end{aligned} \tag{30}$$

Φ_r, Φ_s are in (27), and Φ_r^*, Φ_s^* are in (28). The subsequent subsection will analyze the error convergence and the H-infinity criterion.

4.3. Analysis of the error convergence and the H-infinity criterion

From (19), the following supposition is considered.

S1: There exists a positive constant $O_\delta > 0$ such that δ_c is bounded as

$$\delta_c^T \delta_c \leqslant O_\delta^T O_\delta \tag{31}$$

and $\delta_c = \delta + q - \delta_\Phi, q$ is in (17), δ is in (22), and $\delta_\Phi = \left(\widetilde{\Phi}_r^T + \widetilde{\Phi}_r^T\right)\Psi(\chi)$.

The following theorem is used to satisfy the error convergence and the H-infinity criterion.

Theorem 1. *Take into account that* **S1** *is satisfied, the controller law is described by Eqs. (20), (25) with the dead-zone adapting laws*

$$\begin{aligned} \dot{\Phi}_r &= \left\{ \begin{matrix} -\Delta_r e_c^T P_c B_c \Psi(\chi) if \|\Phi_r\| < k_{\Phi_r} \\ 0 |\Phi_r| \geqslant k_{\Phi_r} \end{matrix} \right\}, \\ \dot{\Phi}_s &= \left\{ \begin{matrix} -\Delta_s e_c^T P_c B_c \Psi(\chi) if \|\Phi_s\| < k_{\Phi_s} \\ 0 |\Phi_s| \geqslant k_{\Phi_s} \end{matrix} \right\}, \end{aligned} \tag{32}$$

assures that the tracking error e_c is uniformly convergent, and the H-infinity criterion (19) is satisfied.

Proof. Define the Lyapunov mapping as

$$W_c = \frac{1}{2} e_c^T P_c e_c + \frac{1}{2\Delta_r}\widetilde{\Phi}_r^T \widetilde{\Phi}_r + \frac{1}{2\Delta_s}\widetilde{\Phi}_s^T \widetilde{\Phi}_s. \tag{33}$$

The derivative is

$$\dot{W}_c = \frac{1}{2}\dot{e}_c^T P_c e_c + \frac{1}{2} e_c^T P_c \dot{e}_c + \frac{1}{\Delta_r}\widetilde{\Phi}_r^T \dot{\widetilde{\Phi}}_r + \frac{1}{\Delta_s}\widetilde{\Phi}_s^T \dot{\widetilde{\Phi}}_s. \tag{34}$$

Substituting (23) in (34) it is

$$\begin{aligned}&\dot{W}_c = \tfrac{1}{2}e_c^T\left\{A_c^TP_c + P_cA_c\right\}e_c\\&+e_c^TP_cB_c(u_c+\delta+q) + \tfrac{1}{\Delta_r}\widetilde{\Phi}_r^T\dot{\widetilde{\Phi}}_r + \tfrac{1}{\Delta_s}\widetilde{\Phi}_s^T\dot{\widetilde{\Phi}}_s.\end{aligned} \tag{35}$$

Now, employing the positive semi-definite matrix Q_c, then there exists a positive definite matrix P_c, such that they are solutions of the matrix equation

$$A_c^TP_c + P_cA_c - P_cB_c\left(\frac{2}{\psi} - \frac{1}{\lambda^2}\right)B_c^TP_c = -Q_c. \tag{36}$$

Substituting the Eq. (36) into (35) results in

$$\begin{aligned}&\dot{W}_c = -\tfrac{1}{2}e_c^TQ_ce_c + \tfrac{1}{2}e_c^TP_cB_c\left(\tfrac{2}{\psi}-\tfrac{1}{\lambda^2}\right)B_c^TP_ce_c\\&+e_c^TP_cB_c\left(-\tfrac{1}{\psi}B_c^TP_ce_c\right) + e_c^TP_cB_c(\delta+q)\\&+\tfrac{1}{\Delta_r}\widetilde{\Phi}_r^T\dot{\widetilde{\Phi}}_r + \tfrac{1}{\Delta_s}\widetilde{\Phi}_s^T\dot{\widetilde{\Phi}}_s.\end{aligned} \tag{37}$$

From (30)$\dot{\widetilde{\Phi}}_r = \dot{\Phi}_r - \dot{\Phi}_r^* = \dot{\Phi}_r$ and $\dot{\widetilde{\Phi}}_s = \dot{\Phi}_s - \dot{\Phi}_s^* = \dot{\Phi}_s$, and substituting (32) into (37) results in

$$\begin{aligned}&\dot{W}_c = -\tfrac{1}{2}e_c^TQ_ce_c - \tfrac{1}{2\lambda^2}e_c^TP_cB_cB_c^TP_ce_c\\&+e_c^TP_cB_c(\delta+q) - e_c^TP_cB_c\left(\widetilde{\Phi}_r^T + \widetilde{\Phi}_s^T\right)\Psi(\chi),\\&= -\tfrac{1}{2}e_c^TQ_ce_c - \tfrac{1}{2\lambda^2}e_c^TP_cB_cB_c^TP_ce_c\\&+e_c^TP_cB_c(\delta+q) - e_c^TP_cB_c\delta_\Phi,\\&= -\tfrac{1}{2}e_c^TQ_ce_c - \tfrac{1}{2\lambda^2}e_c^TP_cB_cB_c^TP_ce_c\\&+e_c^TP_cB_c(\delta+q-\delta_\Phi),\end{aligned} \tag{38}$$

$\delta_\Phi = \left(\widetilde{\Phi}_r^T + \widetilde{\Phi}_r^T\right)\Psi(\chi)$. Making $\delta_c = \delta + q - \delta_\Phi$, it is

$$\dot{W}_c = -\frac{1}{2}e_c^TQ_ce_c - \frac{1}{2\lambda^2}e_c^TP_cB_cB_c^TP_ce_c + e_c^TP_cB_c\delta_c. \tag{39}$$

(39) is rewritten as

$$\dot{W}_c = -\frac{1}{2}e_c^TQ_ce_c - \frac{1}{2\lambda^2}e_c^TP_cB_cB_c^TP_ce_c + e_c^TP_cB_c\delta_c. \tag{40}$$

The last two terms of (40) satisfy the matrix inequality

$$-\frac{1}{2\lambda^2}e_c^TP_cB_cB_c^TP_ce_c + e_c^TP_cB_c\delta_c \leqslant \frac{1}{2}\lambda^2\delta_c^T\delta_c. \tag{41}$$

Substituting (41) into (40) and using (31) is

$$\begin{aligned}&\dot{W}_c \leqslant -\tfrac{1}{2}e_c^TQ_ce_c + \tfrac{1}{2}\lambda^2\delta_c^T\delta_c.\\&\dot{W}_c \leqslant -\tfrac{1}{2}e_c^TQ_ce_c + \tfrac{1}{2}\lambda^2O_\delta^TO_\delta.\end{aligned} \tag{42}$$

From the Eq. (23), supposition **S1**, and references [25–30], yields that the tracking error e_c is uniformly convergent.

Integrating (42) from 0 to t is

$$\begin{aligned}&\textstyle\int_0^t \dot{W}_c dt \leqslant -\tfrac{1}{2}\int_0^t e_c^TQ_ce_c dt + \tfrac{1}{2}\lambda^2\int_0^t O_\delta^TO_\delta dt\\&\Rightarrow W_c(t) - W_c(0) \leqslant -\tfrac{1}{2}\int_0^t e_c^TQ_ce_c dt + \tfrac{1}{2}\lambda^2\int_0^t O_\delta^TO_\delta dt\\&\Rightarrow \tfrac{1}{2}\int_0^t e_c^TQ_ce_c dt \leqslant \tfrac{1}{2}\lambda^2\int_0^t O_\delta^TO_\delta dt + W_c(0)\end{aligned} \tag{43}$$

Applying $\lim_{t\to\infty}\frac{2}{t}$ to both sides of (43) is

$$\begin{aligned}&\lim_{t\to\infty}\tfrac{1}{t}\int_0^t e_c^TQ_ce_c dt \leqslant \lim_{t\to\infty}\tfrac{1}{t}\lambda^2\int_0^t O_\delta^TO_\delta dt + \lim_{t\to\infty}\tfrac{2}{t}W_c(0)\\&\lim_{t\to\infty}\tfrac{1}{t}\int_0^t e_c^TQ_ce_c dt \leqslant \lambda^2\lim_{t\to\infty}\tfrac{1}{t}\int_0^t O_\delta^TO_\delta dt\end{aligned} \tag{44}$$

Finally, since (44) is (19), the H-infinity criterion (19) is satisfied.

Remark 3. Parameters in the Maglev model (11) and in transformed Maglev process (15), (16) are selected to better represent the real process. Parameters of the controller (20), (25) are selected to satisfy (36) and to satisfy that the polynomial (20) is Hurwitz.

Remark 4. The main equations of the adapting strategy are (26), (32), and the main equations of the H-infinity controller are (20), (25). Thus the main equations of the adapting H-infinity controller for the desired reference tracking of the sphere position in the Maglev process are (26), (32), (20), (25).

Remark 5. From (26), (32), (20), (25), the variables of the adapting H-infinity controller are described as following: $\chi = [\chi_1, \chi_2, \chi_3]^T$ is the main variables of the Maglev process (11), $e_c = \left[\tilde{y}, \dot{\tilde{y}}, \ddot{\tilde{y}}\right]^T$ is the tracking error, $\zeta^T = [\zeta_0, \zeta_1, \zeta_2]$ is the proportional gain of the controller, $P_c \in \Re^{3\times3}$, $Q_c \in \Re^{3\times3}$ are matrices to satisfy the error convergence analysis and the H-infinity criterion, Δ_r, Δ_s are the gains of the adapting strategy, $\tilde{y} = \varsigma y - \varsigma y_d$ is the output tracking error, ςy_d is the desired reference, u^* is the steady controller, χ_1^* is the constant equilibrium points of the position, ςu is the input, and $\varsigma y = \varsigma\chi_1 + \chi_1^*$ is the output of the transformed Maglev process (15), (16), $\hat{r}(\chi), \hat{s}(\chi)$are the estimation of unknown nonlinear mappings $r(\chi), s(\chi), l = \overline{1,n}, i = \overline{1,2}, \mu_{M_l} = e^{-\left(\frac{\chi - c_l}{\sigma_l}\right)^2}$ are Gaussian mappings, c_l are centers, σ_l are widths, Φ_r, Φ_s are variables of the adapting strategy, $\hat{\Phi}_r(0) = 0, \hat{\Phi}_s(0) = 0$, $\zeta_0 \in [0, 500]$, $\zeta_1 \in [0, 500]$, $\zeta_2 \in [0, 500]$, $B_c = [0, 0, 1]^T$, $\Delta_r \in [0, 1], \Delta_s \in [0, 1], \psi \in [0, 1], \lambda \in [0, 1]$, c_l=[rand, rand, rand]^T, σ_l=rand, rand is a random number between 0 and 1.

Remark 6. The main goal of the adapting H-infinity controller (26), (32), (20), (25) is that the process output $\varsigma y = \varsigma\chi_1 + \chi_1^*$ (15), (16) must reach the bounded desired reference ςy_d which is denoted as the desired reference tracking of the sphere position in the Maglev process. Thus, the main variables which influence the performance of the adapting H-infinity controller are $P_c \in \Re^{3\times3}$, $Q_c \in \Re^{3\times3}$ which must solve the Eq. (36) to satisfy the error convergence analysis and the H-infinity criterion, the proportional gain of the controller $\zeta^T = [\zeta_0, \zeta_1, \zeta_2]$ which directly affect the tracking error $e_c = \left[\tilde{y}, \dot{\tilde{y}}, \ddot{\tilde{y}}\right]^T$ in the Eq. (20) to improve the controller performance, and the gains of the adapting strategy Δ_r, Δ_s in the equation which directly affect the output of the adapting strategy $\hat{r}(\chi), \hat{s}(\chi)$(32) to improve the estimation performance.

Remark 7. There are three differences between the introduced strategy and studies of [1,6,7,13,16]. The first difference is that in this research the Foucault current is introduced for the description of vibrations in the sphere position, while in previous studies vibrations are considered as disturbances. The second difference is that in this research a dead-zone is introduced in adapting laws to assure the tracking error convergence and H-infinity criterion, while previous studies only assure the tracking error convergence. The third difference is that previous studies consider only the desired reference tracking of fast dynamics, while this research considers the desired reference tracking of fast and slow dynamics.

5. Simulations

In this section, to show the effectiveness of the adapting H-infinity controller, it is compared with the two stages controller of [14,15] and with the robust tracking controller of [16,17] for the desired reference tracking of the sphere position in the Maglev process. Investigations of [14–16], [17] are utilized for comparisons because both techniques are applied for the desired reference tracking of the sphere position in the Maglev process. All parameters are selected for optimum process behavior. The Maglev process of (11) is

$$\begin{aligned} \dot{\chi}_1 &= \chi_2, \\ \dot{\chi}_2 &= -\frac{L_r}{2am}\chi_3^2 e^{-\frac{\chi_1}{a}} + g, \\ \dot{\chi}_3 &= \frac{k_i u}{L_0 + L_r e^{-\frac{\chi_1}{a}}} - \frac{R\chi_3}{L_0 + L_r e^{-\frac{\chi_1}{a}}} + \frac{c_i}{L_0 + L_r e^{-\frac{\chi_1}{a}}}, \\ y &= \chi_1. \end{aligned} \tag{45}$$

Table 1 shows the parameters of the Maglev process and the variables ideally take values in the intervals $\chi_1 \in [0, 0.016]$, $\chi_2 \in [-\infty, \infty], \chi_3 \in [0.03884, 2.38]$, and $u \in [0, 1]$. Parameters are selected such as the model behavior is near to that of the real process.

We utilize the root mean square error (Error) for the comparisons as

$$Error = \left(\frac{1}{T}\int_0^{TF} (e_c^T e_c)dt\right)^{\frac{1}{2}}, \tag{46}$$

Table 1
Parameters of the Maglev process.

Parameters	Values
m	0.0571kg
g	9.81 $\frac{m}{s^2}$
L_r	0.017521H
L_0	0.038514H
a	0.005831m
c_i	0.0243V
k_i	2.5165

$e_c = \left[\tilde{y}, \dot{\tilde{y}}, \ddot{\tilde{y}}\right]^T$ is the tracking error, $\tilde{y} = \varsigma y - \varsigma y_d$ is the output tracking error described in (20), and TF is the final time.

5.1. Two stages controller

In [14,15], a controller is proposed as the combination of a neural network and a sliding mode technique, it is called a two stages controller. The controller law is

$$u = s^* u_1 + (1 - s^*)u_2, \tag{47}$$

$u_1 = \phi - A\chi^* - W\sigma(\widehat{\chi})$, $u_2 = -k_1|\Delta_i^*|sign(\Delta_i^*) + d_i, \dot{d}_i = -k_2 sign(\Delta_i^*)$, with the adapting law

$$\dot{W} = -s^* K_1 P \sigma(\chi)\Delta_t^T, \tag{48}$$

s^* is the commutation variable which interpolates the neural controller u_1 and the sliding mode controller u_2, W are the parameters of the neural networks, $\sigma(\chi)$are the sigmoid mappings, χ are states of the neural network, and Δ_t is the identification error.

Parameters of the two stages controller are, $\sigma(\chi) = \frac{1}{1+e^{-\chi}}$, $\phi = 0.5\sin(0.06t) + 0.8$, and

$$A = \begin{bmatrix} -10 & 0 \\ 0 & -12 \end{bmatrix}, W(0) = \begin{bmatrix} 1.5 & 7 & 5 \\ 0.5 & 2.8 & 0.8 \\ 10 & 12 & 1 \end{bmatrix}, s^* = \begin{cases} 1 & \text{if } \|\Delta_t^*\|_{Q_1}^2 \geqslant -\gamma \\ 0 & \text{if } \|\Delta_t^*\|_{Q_1}^2 \leqslant -\gamma \end{cases}, P = \begin{bmatrix} 8 & 0.8 & 4 \\ 25 & 5 & 3 \\ 9.4 & 7 & 0.4 \end{bmatrix},$$

$\chi(0) = \left[\chi_1(0), \chi_2(0), \chi_3(0)\right]^T = [0.6, 0, 0]^T$.

Sphere positions of the two stages controller of (45), (47), (48) with the sine and square desired references are shown in Fig. 4 a) and Fig. 4 b), respectively. Errors of (46) in the two stages controller for the sine and square desired references are shown in Fig. 5 a) and Fig. 5 b), respectively.

5.2. Robust tracking controller

In [16,17], the design of the controller satisfies the restriction of the unidirectional controller, i.e., the square of the electric current must be non-negative during the process operation, and it requires the knowledge of disturbance. A second order filter is introduced to obtain the feedback signals for the controller as

$$\begin{aligned} \dot{r} = &-\frac{d\varphi(\chi_1)}{dt}\frac{gtd - \ddot{\chi}_1}{\varphi(\chi_1)} - \varphi(\chi_1)sign(\tau)\dot{\tau} + \dot{d} - \varsigma\dddot{y}_d \\ &+\alpha_1\ddot{e} + \alpha_2\dot{e} - r_f - (k+1)r + e_1 - e_{1f}, \end{aligned} \tag{49}$$

$\varphi(s) = \frac{Q}{2M(\chi_\infty + \chi_1)^2}$, is the input gain which is expressed by the Faraday law. The controller input $\dot{\tau}$ is designed to be a solution of the differential equation

$$\begin{aligned} \dot{\tau} = &\kappa(|r_f| + |e_2|) \\ &+sign(\tau)(-(k+1)r_f + 2\beta sign(e_2)). \end{aligned} \tag{50}$$

Parameters of the robust tracking controller are $M = 0.45$ kg, $\chi_\infty = 0.005261$ m, $Q = 0.001247$ Hm, $d = 0.4\sin(0.5t)ms^2, \alpha_1 = 20, \alpha_2 = 10, \beta = 7$, $k = 180, \kappa = 0.00145, \chi(0) = \left[\chi_1(0), \chi_2(0), \chi_3(0)\right]^T = [0.6, 0, 0]^T$.

Sphere positions of the robust tracking controller of (45), (49), (50) with the sine and square desired references are shown in Fig. 6 a) and Fig. 6 b), respectively. Errors of (46) in the robust tracking controller for the sine and square desired references are shown in Fig. 7 a) and Fig. 7 b), respectively.

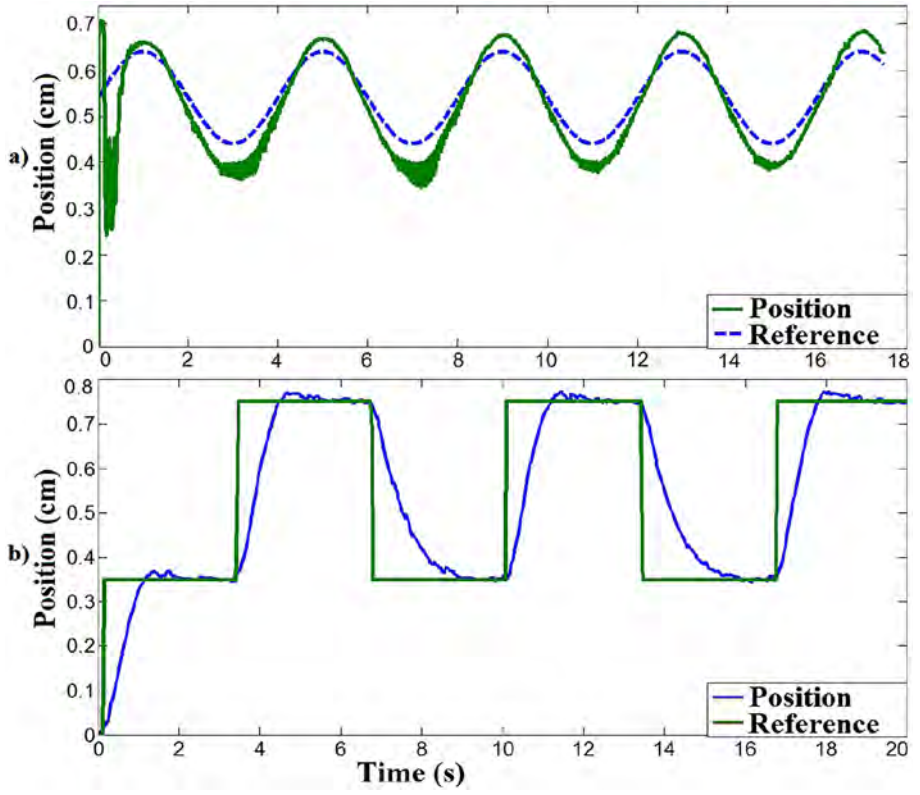

Fig. 4. Sphere positions with the two stages controller.

5.3. Adapting H-infinity controller

In the adapting H-infinity controller, the controller law of (20), (25) is

$$\begin{aligned} u &= u^* + \varsigma u, \\ \varsigma u &= \tfrac{1}{\widehat{s}(\chi)}\left[-\widehat{r}(\chi) + \varsigma \cdot \ddot{y}_d - \zeta^T e_c + u_c\right], \\ u_c &= -\tfrac{1}{\psi} B_c^T P_c e_c, \end{aligned} \tag{51}$$

u^* is selected by user between the values $u^* \in [0,1]$, $\widehat{r}(\chi)$and $\widehat{s}(\chi)$are the estimation of unknown nonlinear mappings $r(\chi)$and $s(\chi)$used to find $\varsigma u, \chi = [\chi_1, \chi_2, \chi_3]^T$ are the main variables of the Maglev process, $e_c = \left[\tilde{y}, \dot{\tilde{y}}, \ddot{\tilde{y}}\right]^T$ is the tracking error, $\zeta^T = [\zeta_0, \zeta_1, \zeta_2]$ is the proportional gain of the controller, $\tilde{y} = \varsigma y - \varsigma y_d$ is the output tracking error, ςu and $\varsigma y = \varsigma\chi_1 + \chi_1^*$ are the input and output of the transformed Maglev process, ςy_d is the desired reference, χ_1^* is selected by user between the values $\chi_1^* \in [0, 0.016]$, $B_c = [0,0,1]^T$, and the adapting strategy of (26), (32) is

$$\begin{aligned} \widehat{r}(\chi) &= \Phi_r^T \Psi(\chi), \\ \widehat{s}(\chi) &= \Phi_s^T \Psi(\chi), \\ \Psi(\chi) &= \sum_{l=1}^{49} \mu_{M_l}, \\ \dot{\Phi}_r &= \left\{ \begin{array}{c} -\Delta_r e_c^T P_c B_c \Psi(\chi) if ||\Phi_r|| < k_{\Phi_r} \\ 0 ||\Phi_r|| \geqslant k_{\Phi_r} \end{array} \right\}, \\ \dot{\Phi}_s &= \left\{ \begin{array}{c} -\Delta_s e_c^T P_c B_c \Psi(\chi) if ||\Phi_s|| t < k_{\Phi_s} \\ 0 ||\Phi_s|| \geqslant k_{\Phi_s} \end{array} \right\}, \end{aligned} \tag{52}$$

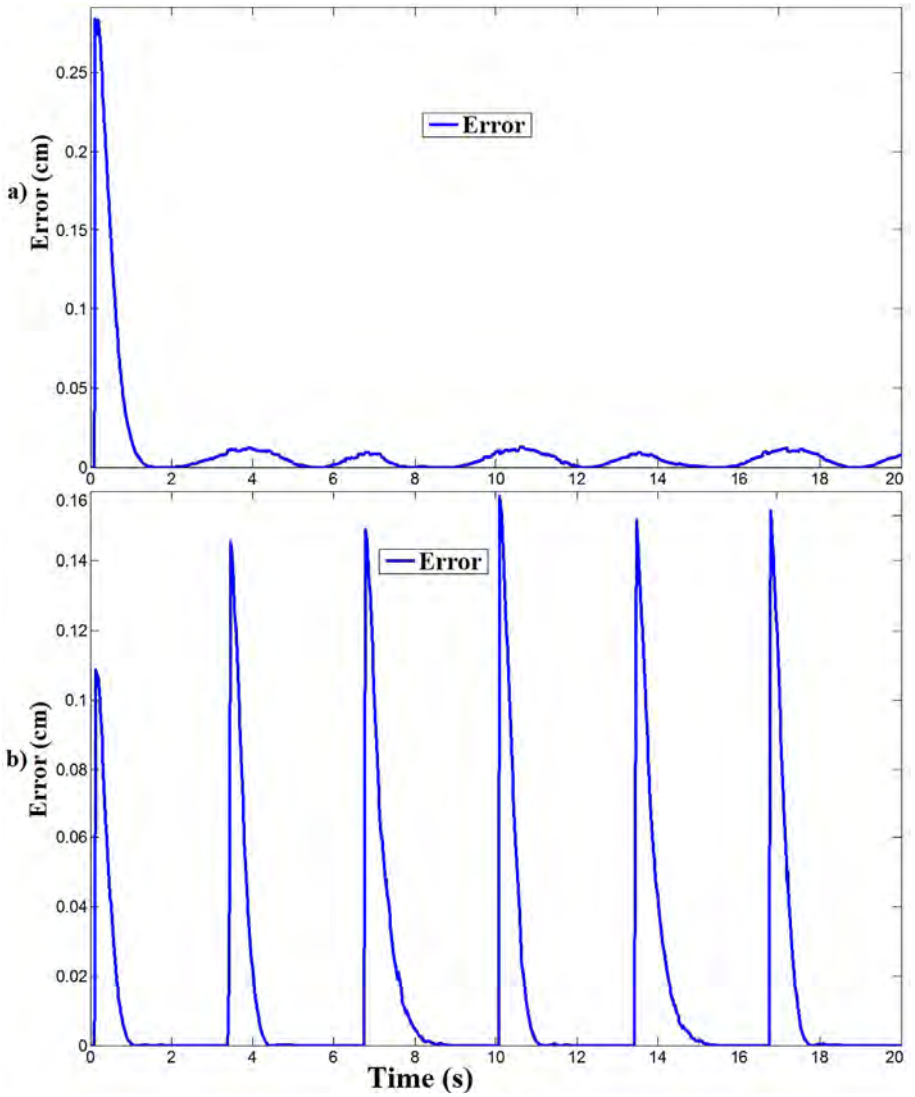

Fig. 5. Errors of the two stages controller.

$l = \overline{1,49}, \mu_{M_l} = e^{-\left(\frac{\chi - c_l}{\sigma_l}\right)^2}$ are Gaussian mappings, c_l are centers, σ_l are widths, $\hat{r}(\chi), \hat{s}(\chi)$are outputs of the adapting strategy, $\chi = [\chi_1, \chi_2, \chi_3]^T$. Φ_r, Φ_s are variables of the adapting strategy. Parameters of the adapting H-infinity controller are $u^* = 0.5, \chi_1^* = 0.01, \Delta_r = 0.028$, $\Delta_s = 0.215, \psi = 0.1, \lambda = 0.325, l = \overline{1,49}$, $i = \overline{1,2}, c_l$=[rand, rand, rand]^T, σ_l=rand, rand is a random number between 0 and 1, $\widehat{\Phi}_r(0) = 0, \widehat{\Phi}_s(0) = 0$, and

$$P_c = \begin{bmatrix} 10 & 1 & 1 \\ 1 & 0.5 & 0.8 \\ 12 & 4 & 1 \end{bmatrix}, Q_c = \begin{bmatrix} 42.6 & 4.02 & 1 \\ 4.02 & 1.63 & 2 \\ 30 & 2 & 1 \end{bmatrix}, \zeta = [\zeta_0, \zeta_1, \zeta_2]^T = [100, 70, 12]^T, \chi(0) = [\chi_1(0), \chi_2(0), \chi_3(0)]^T = [0.6, 0, 0]^T.$$

Parameters are selected such that this controller reaches an acceptable performance and such that Theorem 1 is maintained because from (52) $\|\hat{r}(\chi)\| \leq 1, \|\hat{s}(\chi)\| \leq 1$, and as $\hat{r}(\chi) = \Phi_r^T \Psi(\chi), \hat{s}(\chi) = \Phi_s^T \Psi(\chi)$, this yields that $\|\Phi_r\| \leqslant k_{\Phi_r}, \|\Phi_s\| \leqslant k_{\Phi_s}$ of the condition (32) is assured.

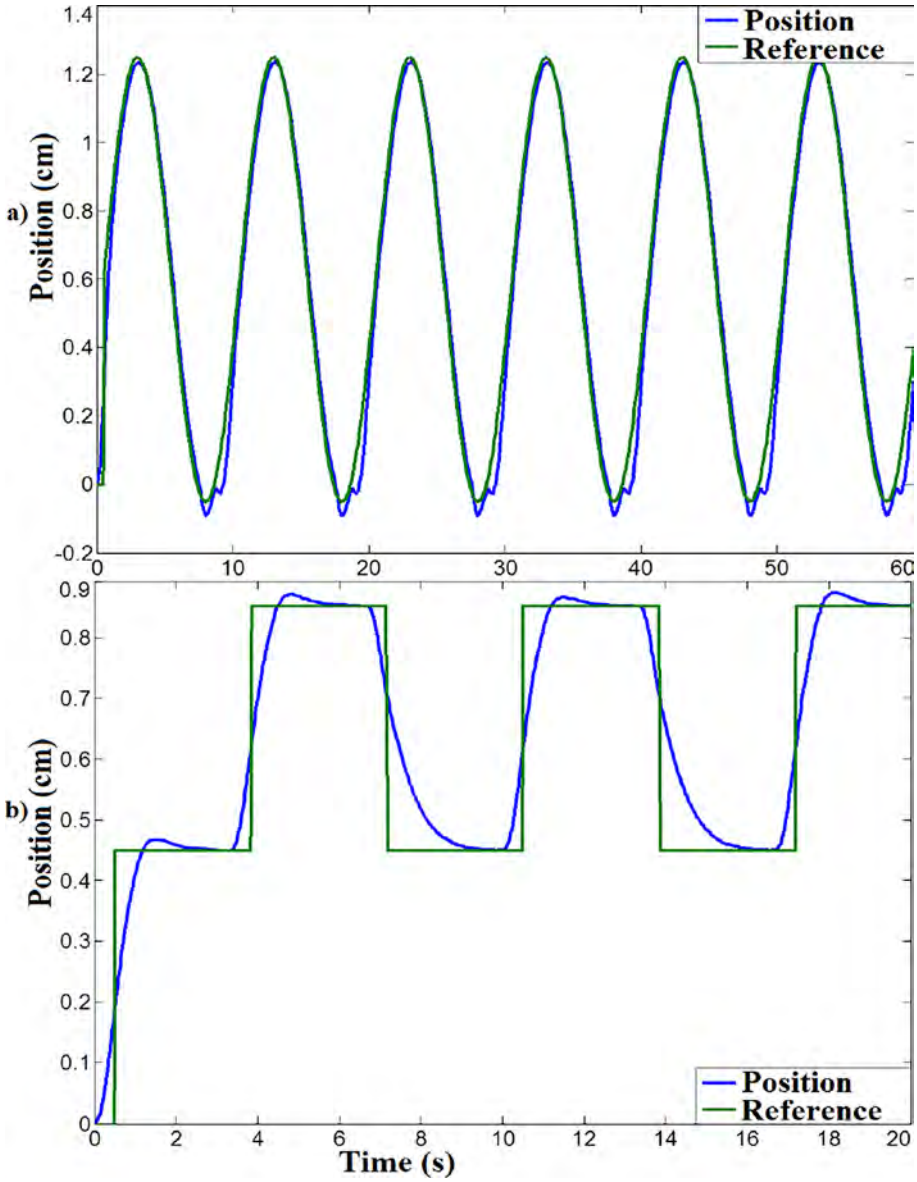

Fig. 6. Sphere positions with the robust tracking controller.

Sphere positions of the adapting H-infinity controller of (45), (51), (52), for the sine and square desired references are shown in Fig. 8 a) and Fig. 8 b), respectively. And Errors of (46) in the adapting H-infinity controller for the sine and square desired references are shown in Fig. 9 a) and Fig. 9 b), respectively.

5.4. Comparisons

From Fig. 4 and Fig. 5, it is shown that the two stages controller of (45), (47), (48) and [14,15] does not demonstrate to reach a good desired reference tracking of the sphere position; it is because in the two stages controller, the Foucault current is not considered. From Fig. 6 and Fig. 7, it is shown that the robust tracking controller of (45), (49), (50) and [16,17] reaches a better desired reference tracking of the sphere position than the two stage controller, but it still could be improved. On the other hand, from Fig. 8 and Fig. 9, it can be observed that the adapting H-infinity controller of (45), (51), (52) obtains a better desired reference tracking of the sphere position than both the two stages and robust tracking controllers because the error signals in the adapting H-infinity controller converge to zero faster than in the other two controllers.

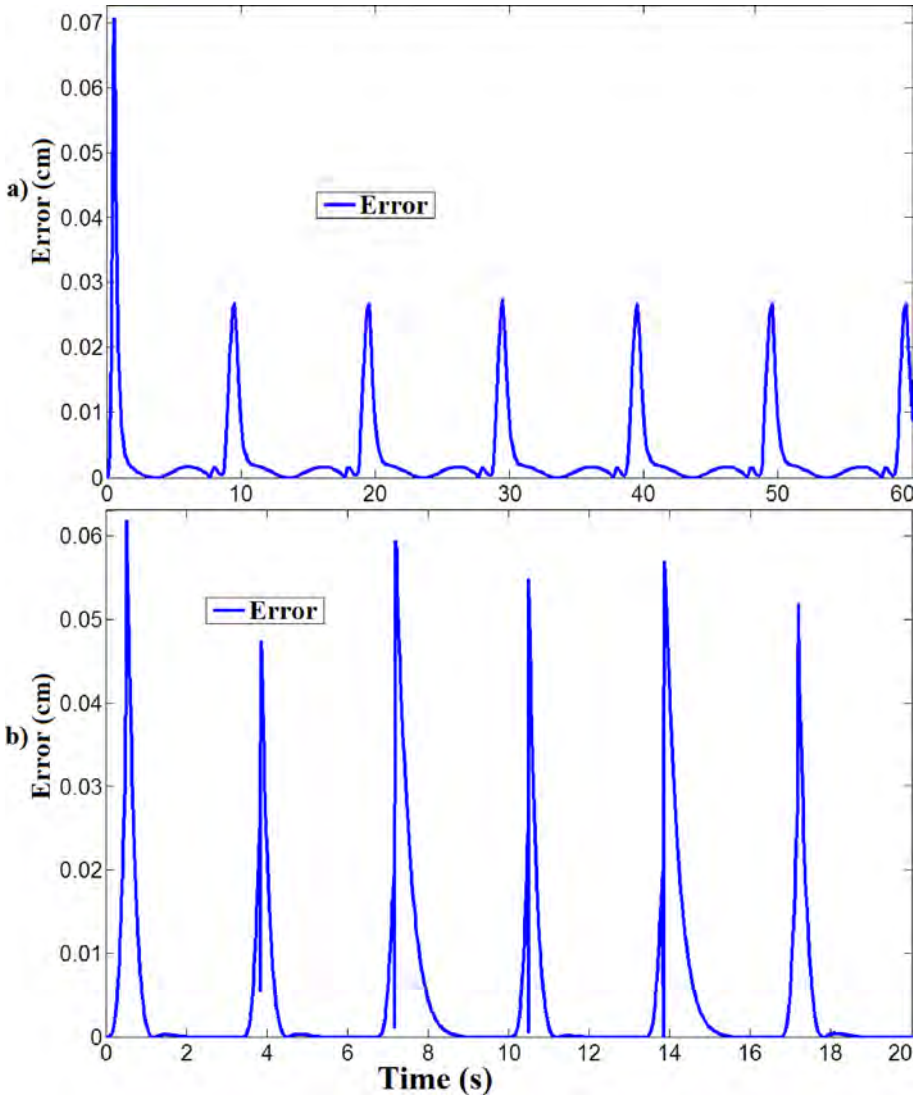

Fig. 7. Errors of the robust tracking controller.

Furthermore, Table 2 shows the comparison results for the desired reference tracking of the sphere position in the adapting H-infinity controller of (45), (51), (52), the two stages controller of Eqs. (45), (47), (48), and robust tracking controller of (45), (49), (50) based on the root mean square error (Error) of (46) and the first improves both the second and the third because the Error of the first is smaller than of the other two.

6. Conclusion

In this research, an adapting H-infinity controller was proposed to attenuate the effects of the Foucault current and to improve the desired reference tracking of the sphere position in a Maglev process. The Lyapunov method was utilized to analyze the error convergence and the H-infinity criterion of the proposed method. The proposed strategy could be applied for the desired reference tracking of other mechatronic processes such as robots, cranes, or pendulums. Finally, the adapting H-infinity controller was compared with both the two stages and robust tracking controllers yielding that the adapting H-infinity controller showed the best desired reference tracking because the sphere position reached the desired reference quicker and more smoothly, and because the root mean square error for the adapting H-infinity controller was the smallest. In the forthcoming work, a Maglev process with more degrees of freedom will be considered, or the proposed strategy will be applied to other kind of mechatronic processes.

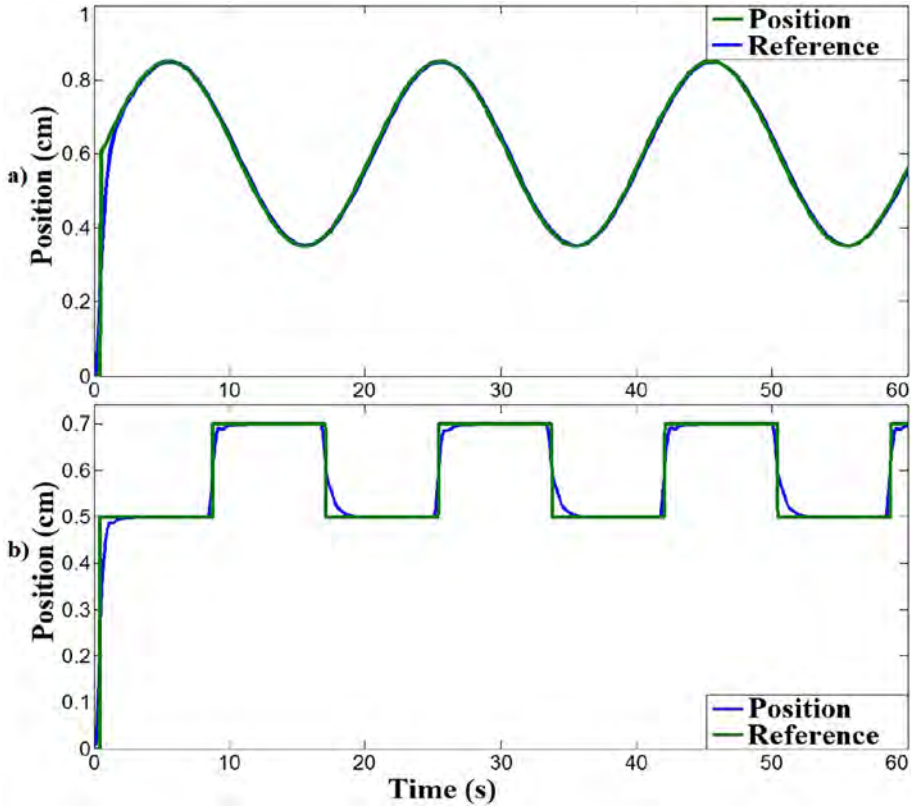

Fig. 8. Sphere positions with the adapting H-infinity controller.

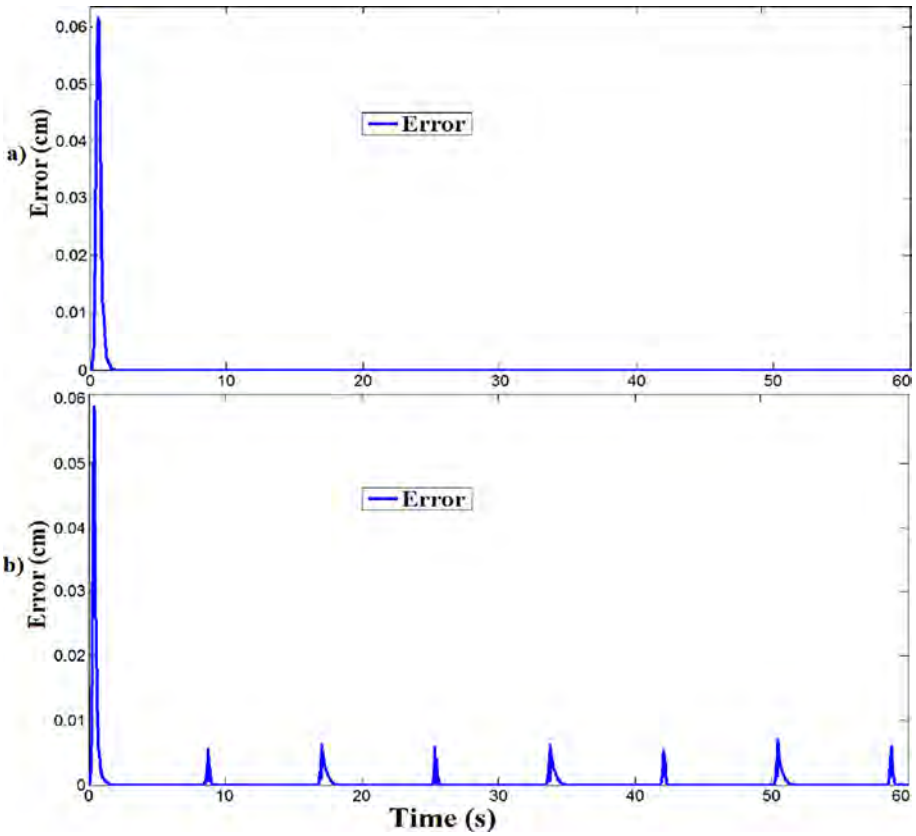

Fig. 9. Errors of the adapting H-infinity controller.

Table 2
Comparison results of the Error.

Signal type	Sine	Square
Two stages	1.461×10^{-1}	6.846×10^{-1}
Robust tracking	5.894×10^{-3}	2.0653×10^{-3}
Adapting H-infinity	3.945×10^{-6}	7.07×10^{-6}

Declaration of Competing Interest

The authors declare that they have no known competing financial interests or personal relationships that could have appeared to influence the work reported in this paper.

Acknowledgment

The authors thank the Secretaría de Investigación y Posgrado, the Comisión de Operación y Fomento de Actividades Académicas, and the Consejo Nacional de Ciencia y Tecnología for their help in this research. The second author acknowledges the support of the Austrian COMET-K2 programme of the Linz Center of Mechatronics (LCM), funded by the Austrian federal government and the federal state of Upper Austria. This publication reflects only the authors views.

References

[1] A.S. Abdelmageed Mahmoud, M. Khan, A.S. Siddique, Discrete-time control of Maglev system using switched fuzzy controller, India Conference, 2015..
[2] R.-C. David, C.-A. Dragos, R.-G. Bulzan, R.-E. Precup, E.M. Petriu, M.-B. Radac, An Approach to Fuzzy Modeling of Magnetic Levitation Systems, Int. J. Artif. Intell. 9 (A12) (2012) 1–18.
[3] J. Zhang, X. Wang, X. Shao, Design and Real-Time Implementation of Takagi-Sugeno Fuzzy Controller for Magnetic Levitation Ball System, IEEE Access 8 (2020) 38221–38228.
[4] W. Zhang, W. Wei, Disturbance-observer-based finite-time adaptive fuzzy control for non-triangular switched nonlinear systems with input saturation, Inf. Sci. 561 (2021) 152–167.
[5] C.-A. Bojan-Dragos, M.-B. Radac, R.-E. Precup, E.-L. Hedrea, O.-M. Tanasoiu, Gain-Scheduling Control Solutions for Magnetic Levitation Systems, Acta Polytechnica Hungarica 15 (5) (2018) 89–108.
[6] M. Khan, A.S. Siddiqui, A.S. Abdelmageed Mahmoud, Robust H_∞ control of magnetic levitation system based on parallel distributed compensator, Ain Shams Eng. J. 9 (4) (2018) 1119–1129.
[7] J.M. Kim, S.H. Lee, Y.K. Choi, Decentralized H_∞ control of Maglev systems, Ann. Conf. Ind. Electron. (2006) 418–423.
[8] W. Yang, F. Meng, M. Sun, K. Liu, Passivity-Based Control Design for Magnetic Levitation System, Appl. Sci. 10 (2020) 2392.
[9] J.S. Lim, H.-W. Lee, Movement Control Method of Magnetic Levitation System Using Eccentricity of Non-Contact Position Sensor, Appl. Sci. 11 (2021) 2396.
[10] F. Ni, Q. Zheng, J. Xu, G. Lin, Nonlinear Control of a Magnetic Levitation System Based on Coordinate Transformations, IEEE Access 7 (2019) 164444–164452.
[11] W. Xia, Z. Long, F. Dou, Disturbance Rejection Control Using a Novel Velocity Fusion Estimation Method for Levitation Control Systems, IEEE Access 8 (2020) 173092–173102.
[12] M. Zhai, Z. Long, X. Li, Fault-Tolerant Control of Magnetic Levitation System Based on State Observer in High Speed Maglev Train, IEEE Access 7 (2019) 31624–31633.
[13] A.V. Starbino, S.S., Design of sliding mode controller for magnetic levitation system, Computers and Electrical Engineering, 78 (2019) 184-203..
[14] W. Yu, P. Cruz, X. Li, Two-stage neural sliding-mode control of magnetic levitation in minimal invasive surgery, Neural Comput. Appl. 20 (2011) 1141–1147.
[15] Y. Zhang, F. Wang, F. Yan, Fast finite time adaptive neural network control for a class of uncertain nonlinear systems subject to unmodeled dynamics, Inf. Sci. 565 (2021) 306–325.
[16] Y. Zhang, B. Xian, S. Ma, Continuous robust tracking control for magnetic levitation system with unidirectional input constraint, IEEE Trans. Industr. Electron. 62 (9) (2015) 5971–5980.
[17] Q. Li, J. Wei, Q. Gou, Z. Niu, Distributed adaptive fixed-time formation control for second-order multi-agent systems with collision avoidance, Inf. Sci. 564 (2021) 27–44.
[18] J. Zhang, W.-J. Wu, W.-B. Xie, C. Peng, Dimensional-varying integral sliding mode controller design for uncertain Takagi-Sugeno fuzzy systems, Inf. Sci. 565 (2021) 77–90.
[19] A. Ashfahani, M. Pratama, E. Lughofer, Y.-S. Ong, DEVDAN: Deep evolving denoising autoencoder, Neurocomputing 390 (2020) 297–314.
[20] D. Leite, I. Skrjanc, Ensemble of evolving optimal granular experts, OWA aggregation, and time series prediction, Inf. Sci. 504 (2019) 95–112.
[21] E. Lughofer, A.-C. Zavoianu, R. Pollak, M. Pratama, P. Meyer-Heye, H. Zorrer, C. Eitzinger, T. Radauer, On-line anomaly detection with advanced independent component analysis of multi-variate residual signals from causal relation networks, Inf. Sci. 537 (2020) 425–451.
[22] S. Samanta, M. Pratama, S. Sundaram, N. Srikanth, Learning elastic memory online for fast time series forecasting, Neurocomputing 390 (2020) 315–326.
[23] I. Skrjanc, J.A. Iglesias, A. Sanchis, D. Leite, E. Lughofer, F. Gomide, Evolving fuzzy and neuro-fuzzy approaches in clustering, regression, identification, and classification: A Survey, Inf. Sci. 490 (2019) 344–368.
[24] A. Yazdinejad, H. HaddadPajouh, A. Dehghantanha, R.M. Parizi, G. Srivastava, M.-Y. Chen, Cryptocurrency malware hunting: A deep Recurrent Neural Network approach, Appl. Soft Comput. 96 (2020) 106630.
[25] C. Aguiar, D. Leite, D. Pereira, G. Andonovski, I. Skrjanc, Nonlinear modeling and robust LMI fuzzy control of overhead crane systems, J. Franklin Inst. 358 (2021) 1376–1402.
[26] M.M. Ferdaus, M. Pratama, S.G. Anavatti, M.A. Garratt, E. Lughofer, PAC: A novel self-adaptive neuro-fuzzy controller for micro aerial vehicles, Inf. Sci. 512 (2020) 481–505.
[27] M.M. Ferdaus, M. Pratama, S.G. Anavatti, M.A. Garratt, Y. Pan, Generic Evolving Self-Organizing Neuro-Fuzzy Control of Bio-Inspired Unmanned Aerial Vehicles, IEEE Trans. Fuzzy Syst. 28 (8) (2020) 1542–1556.
[28] J.-Y. Hsu, Y.-F. Wang, K.-C. Lin, M.-Y. Chen, J.H.-Y. Hsu, Wind Turbine Fault Diagnosis and Predictive Maintenance Through Statistical Process Control and Machine Learning, IEEE Access 8 (2020) 23427–23439.

[29] L. Oliveira, A. Bento, V.J.S. Leite, F. Gomide, Evolving granular feedback linearization: Design, analysis, and applications, Appl. Soft Comput. 86 (2020) 105927.
[30] R.-E. Precup, P. Angelov, B.S. Jales Costa, M. Sayed-Mouchaweh, An overview on fault diagnosis and nature-inspired optimal control of industrial process applications, Comput. Ind. 74 (2015) 75–94.